Dynamic Modeling and Path Planing of Simple Ground Vehicle

Friday, Jan 22, 2021

Ebu Bekir Çiftçi[1]

[1] ciftcie16@itu.edu.tr , ebubekirciftci@yahoo.com

Content

Table List

Figure List

1. Part I: Modelling the Vehicle

This section describes the dynamics of the vehicle. The contents of the previous report remained the same. However, some changes have been made in the dynamics of the vehicle and the changes are described in the section number 1.3.

1.1 Ground Vehicle Dynamic Equations

There are many different types of approaches to Ground Vehicle Dynamics. Bicycle approach, which was used by Riekert and Schunck in 1940, was used in this study. This approach is a good approach for analyzing the motion in the horizontal plane if the torque and force values affecting the vehicle are known [1].

1.1.1 Equations of Forces and Moments

In this study, the steer angle, which will enable the Ground Vehicle to be directed, will be applied only to the Front Wheel. In addition, the vehicle is front wheel drive. Forces, velocities and lengths on the vehicle are shown in Figure 1.

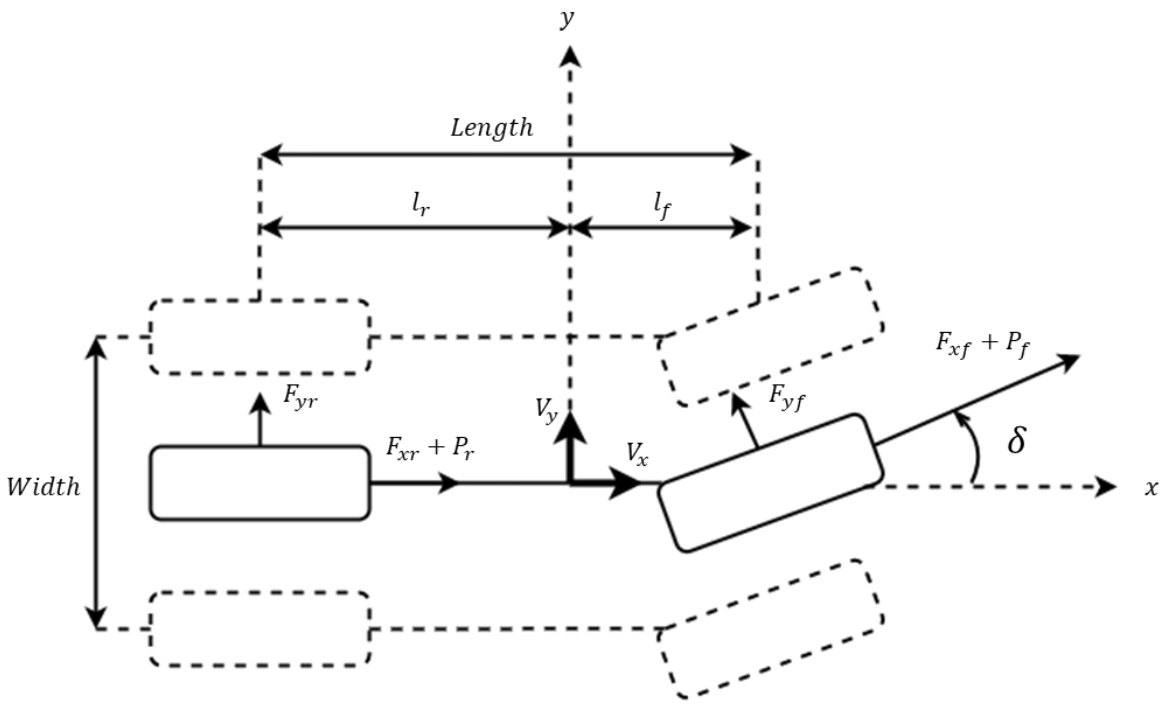

Figure 1: Forces on Body Reference Frame of Bicycle Model

Global position differential equations [2];

$$\dot{X} = V_x \cos\psi - V_y \sin\psi$$
$$\dot{Y} = V_x \sin\psi + V_y \cos\psi \quad (1.1)$$

Force and moment equations with small angle theorem for steer angle [3];

$$I_{zz}\ddot{\psi} = l_f P_f \delta + l_f F_{yf} - l_r F_{yr}$$
$$m\left(\dot{V}_y + \dot{\psi} \times V_x\right) = P_f \delta + F_{yf} + F_{yr} \quad (1.2)$$
$$m\left(\dot{V}_x + \dot{\psi} \times V_y\right) = P_f + P_r + F_{yf}\delta$$

Where;

F_{yr} = Lateral rear tire force

F_{yf} = Lateral front tire force

F_{xr} = Longitudinal rear tire force

F_{xf} = Longitudinal front tire force

P_f = Longitudinal force that on front tire from motor torque

P_r = Longitudinal force that on rear tire from motor torque

V_y = Lateral velocity of vehicle in body reference frame

V_x = Longitudinal velocity of vehicle in body reference frame

Y = Lateral position of vehicle in Inertial Reference frame

X = Longitudinal position of vehicle in Inertial Reference frame

y = Lateral axis of body reference frame

x = Longitudinal axis of body reference frame

δ = Steer Angle

ψ = Yaw Angle

l_r = Vehicle center of gravity location from rear axle

l_f = Vehicle center of gravity location from front axle

$m =$ Vehicle mass

$I_{zz} =$ Vehicle yaw inertia

However, in this study, since the wheel of the vehicle is considered to be rigid, lateral and longitudinal forces arising from the elastic properties of the wheel are neglected. Also, since the vehicle is front-wheel drive, the driving force at the rear wheel is considered zero. Therefore; F_{yr}, F_{yf}, F_{xr}, F_{xf} and P_r are zero. Thus, when force and moment equations are rearranged according to these assumptions;

$$\begin{aligned} I_{zz}\ddot{\psi} &= l_f P_f \delta \\ m\left(\dot{V}_y + \dot{\psi} \times V_x\right) &= P_f \delta \\ m\left(\dot{V}_x + \dot{\psi} \times V_y\right) &= P_f \end{aligned} \tag{1.3}$$

Equation that gives the relationship between the torque of the motor and the force [4];

$$\begin{aligned} P_f &= \tau / R_f \\ \tau &= \frac{\mathbf{V}}{\Omega} k \end{aligned} \tag{1.4}$$

According to Equation 4 that basic DC motor equation; τ Stands for the engine torque, R_f stands for the radius of the front wheel, **V** is input voltage, Ω is electrical resistance and k is motor constant that refer to torque over current.

1.1.2 Equations of Motion

Also results of vector products with respect to global coordinates;

$$\begin{aligned} \dot{\psi} \times V_x &= V_x \dot{\psi} \\ \dot{\psi} \times V_y &= -V_y \dot{\psi} \end{aligned} \tag{1.5}$$

Using equations 3, 4 and 5, equations of motion are expressed as [3];

$$\begin{aligned} \frac{d\dot{\psi}}{dt} &= \frac{l_f \tau \delta}{I_{zz} R_f} \\ \frac{dV_y}{dt} &= \frac{\tau \delta}{m R_f} + V_x \dot{\psi} \\ \frac{dV_x}{dt} &= \frac{\tau}{m R_f} - V_y \dot{\psi} \\ \frac{d\psi}{dt} &= \dot{\psi} \end{aligned} \tag{1.6}$$

Nonlinear state-space model based on Equations 6;

$$\begin{bmatrix} \ddot{\psi} \\ \dot{V}_y \\ \dot{V}_x \\ \dot{\psi} \end{bmatrix} = \begin{bmatrix} 0 & 0 & 0 & 0 \\ 0 & 0 & \dot{\psi} & 0 \\ 0 & -\dot{\psi} & 0 & 0 \\ 1 & 0 & 0 & 0 \end{bmatrix} \begin{bmatrix} \dot{\psi} \\ V_y \\ V_x \\ \psi \end{bmatrix} + \begin{bmatrix} \frac{l_f \delta}{I_{zz} R_f} \\ \frac{\delta}{m R_f} \\ \frac{1}{m R_f} \\ 0 \end{bmatrix} \tau \tag{1.7}$$

τ Input value is output of analytic Equation 4. And last version of state space equations;

$$\dot{x} = \begin{bmatrix} \ddot{\psi} \\ \dot{V}_y \\ \dot{V}_x \\ \dot{\psi} \end{bmatrix} = \begin{bmatrix} 0 & 0 & 0 & 0 \\ 0 & 0 & \dot{\psi} & 0 \\ 0 & -\dot{\psi} & 0 & 0 \\ 1 & 0 & 0 & 0 \end{bmatrix} \begin{bmatrix} \dot{\psi} \\ V_y \\ V_x \\ \psi \end{bmatrix} + \begin{bmatrix} \frac{l_f \delta k}{I_{zz} R_f \Omega} \\ \frac{\delta k}{m R_f \Omega} \\ \frac{k}{m R_f \Omega} \\ 0 \end{bmatrix} \mathbf{V} \tag{1.8}$$

$$y = \begin{bmatrix} 1 & 0 & 0 & 0 \\ 0 & 1 & 0 & 0 \\ 0 & 0 & 1 & 0 \\ 0 & 0 & 0 & 1 \end{bmatrix} \begin{bmatrix} \dot{\psi} \\ V_y \\ V_x \\ \psi \end{bmatrix}$$

1.2 Ground Vehicle Dynamic Calculations

1.2.1 Vehicle Properties

The car used in the study is the vehicle included in the MATLAB Simulink Tool. Vehicle properties are in the Table 1.

Table 1: Vehicle Properties

Features	Values
Mass	$2000\ kg$
Inertia about Z-axis	$4000\ kg/m^2$
Front Axle to Center of Gravity	$1.4\ m$
Rear Axle to Center of Gravity	$1.6\ m$
Radius of front wheel	$0.3\ m$
Motor resistance	$0.02\ ohm$
Motor constant	$1\ Nm/A$

1.2.2 Vehicle Dynamics Model

The dynamic simulation model was made using MATLAB's Simulink tool. As seen in Figure 2, Model, It consists of three main blocks: Input, Outputs and Vehicle Dynamics.

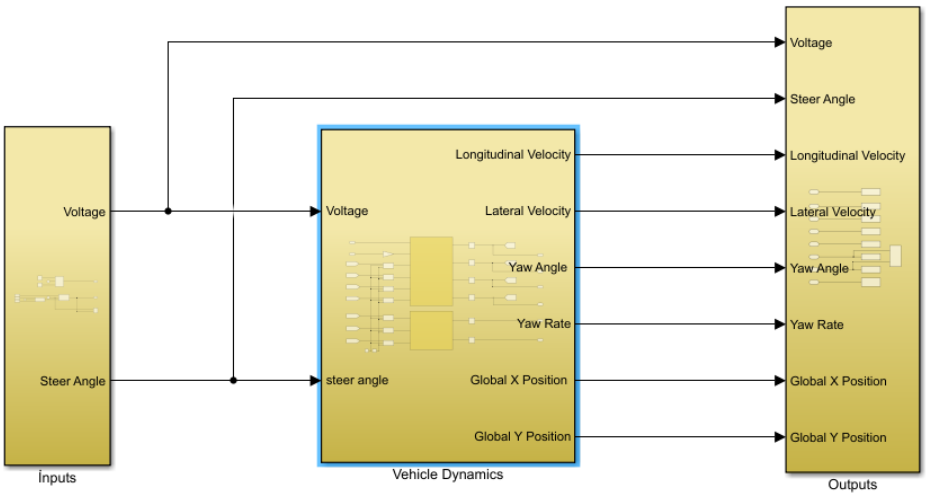

Figure 2: Dynamic Model Main Blocks

The label on which the calculations are made is the Vehicle Dynamics block. There are two function blocks in this block, shown in Figure 3. The "*State Space Subsystem*" block contains the calculation blocks for the nonlinear state-space model equation in Equation 8. Lateral and longitudinal velocity values calculated in this block, velocity values for Inertial Reference Frame are calculated by using the equations in Equation 1 in the "*Global coordinate conversion subsystem*" block. The system is in a loop and the differential expressions, which are the outputs of the system, are integrated and re-inputted into the system. All values are considered zero for initial conditions. However, these initial values can be changed if desired.

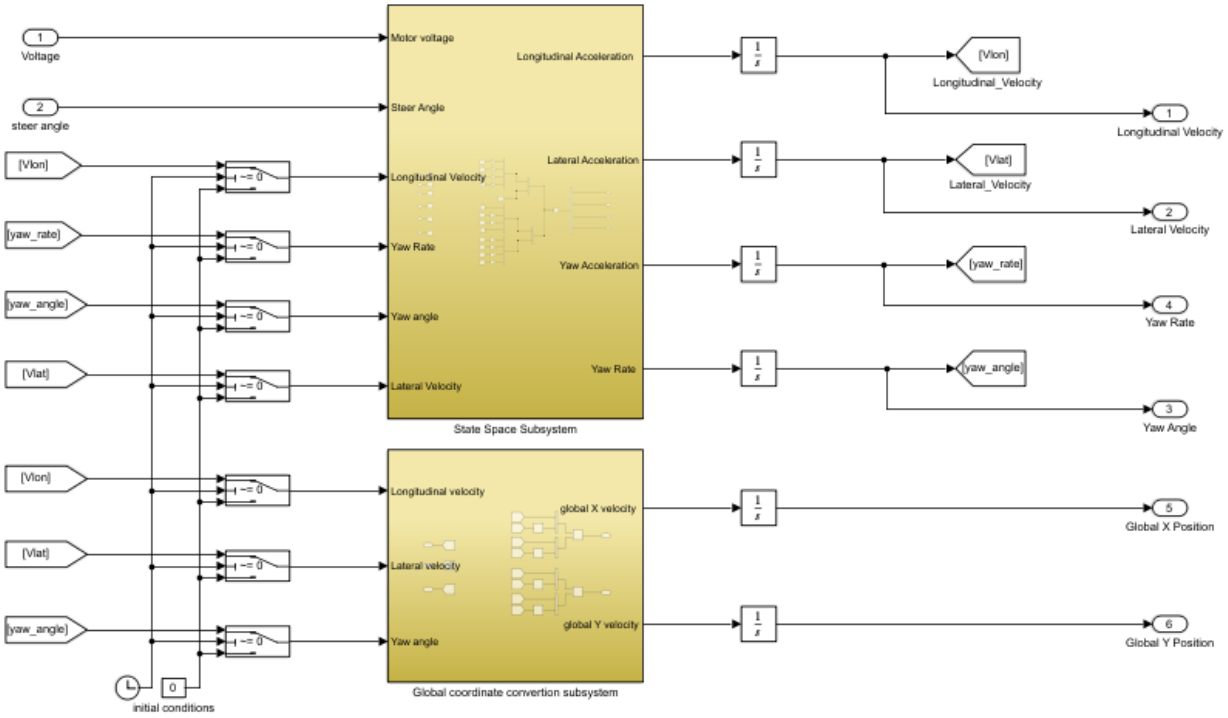

Figure 3: Vehicle Dynamics Block

1.2.3 Results

The dynamic model does not include any controller. For this reason, its control is provided manually, by changing the values of steer angle and motor torque input. Comparison of two different systems with and without manual lateral control will be made in this section.

1.2.3.1 Successful Manual Control

While 10 degree steer angle input was made to the vehicle up to 1.2 seconds, -10 degree steer angle was input up to 2.4 seconds. During the movement of the vehicle (4 seconds), a constant voltage of 120 V was applied to the vehicle. Input graphics are given in Figures 4.

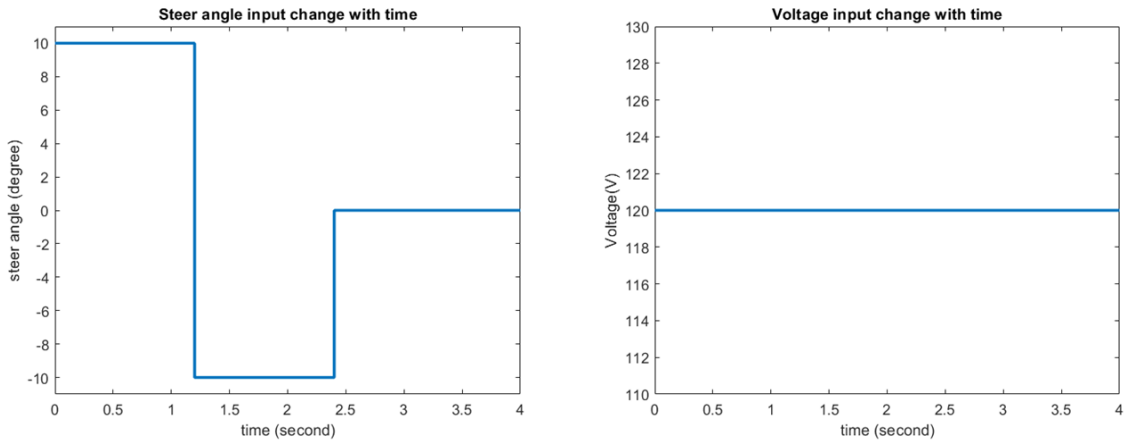

Figure 4: Successful Manual Control Inputs

Lateral and longitudinal velocity outputs in the Body Reference Frame are given in Figure 5. The convergence of the lateral velocity to about 13 meters per second is an indication that lateral control is achieved.

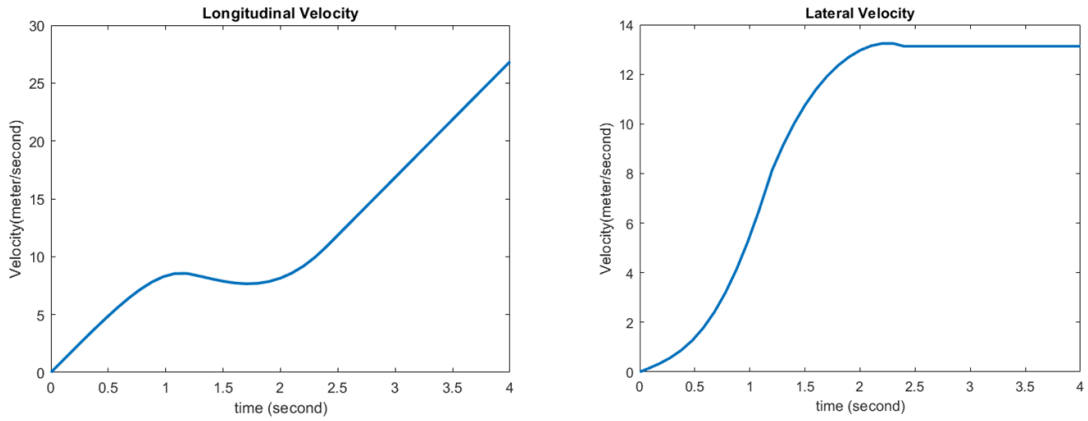

Figure 5: Velocity Outputs of Successful Manual Control

Yaw angle and yaw rate outputs are given in Figure 6. Similarly, the fact that the yaw rate is zero and the yaw angle converge is an indication that lateral control is achieved.

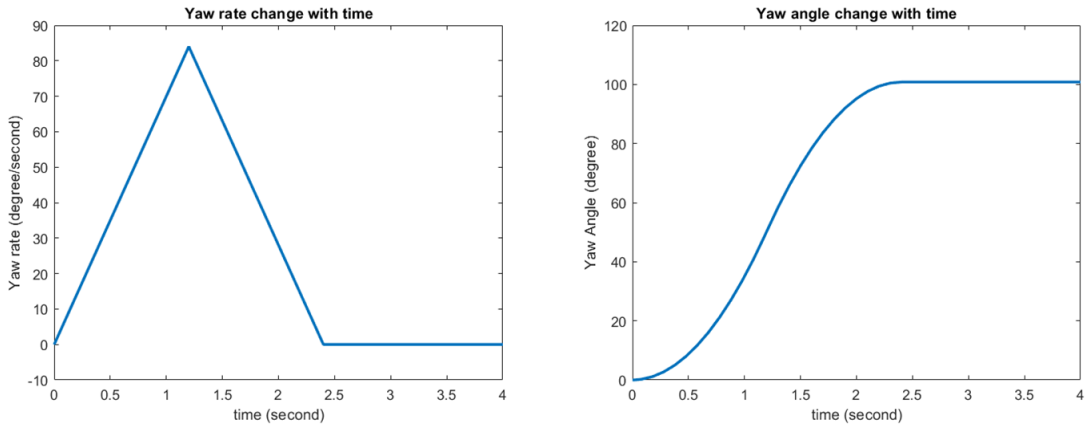

Figure 6: Yaw Outputs of Successful Manual Control

Finally, the change of the vehicle's direction and position with respect to the Inertial Frame is as in Figure 7.

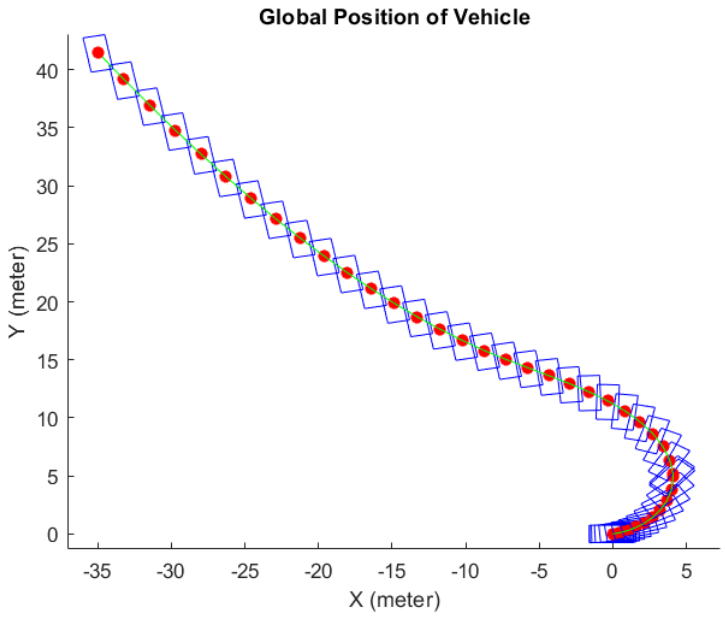

Figure 7: Global Position of Vehicle with Successful Manual Control

1.2.3.2 Unsuccessful Manual Control

While 10 degree steer angle input was made to the vehicle up to 2 seconds, 0 degree steer angle was input up to 4 seconds, after a 2-second 120 V step input, the applied torque is eliminated. Input graphics are given in Figures 8.

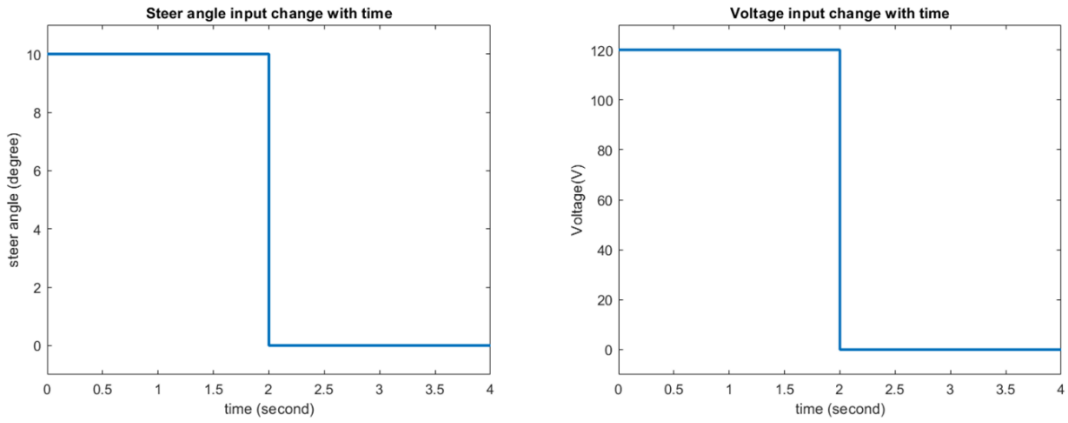

Figure 8: Unsuccessful Manual Control Inputs

Lateral and longitudinal velocity outputs in the Body Reference Frame are given in Figure 9. The fact that the lateral velocity is constantly changing shows that control cannot be achieved.

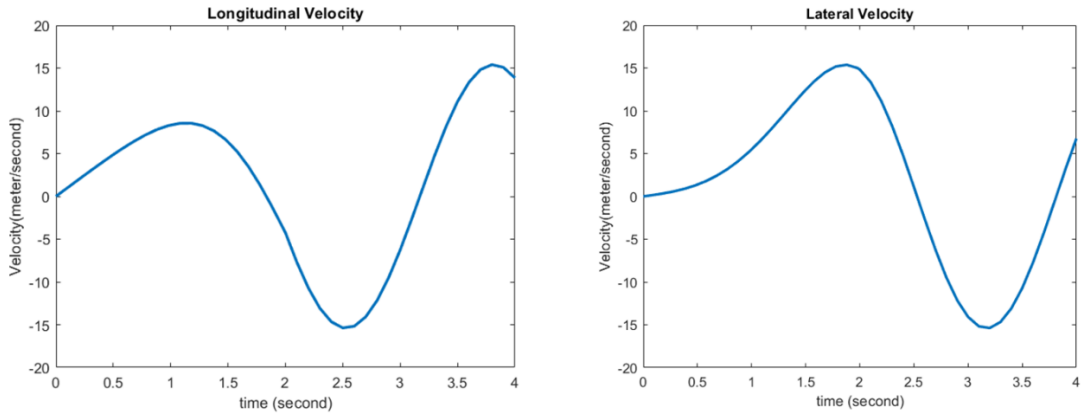

Figure 9: Velocity Outputs of Unsuccessful Manual Control

Yaw angle and yaw rate outputs are given in Figure 10. Similarly, the fact that the yaw rate is not zero and the yaw angle not converge is an indication that lateral control is not achieved.

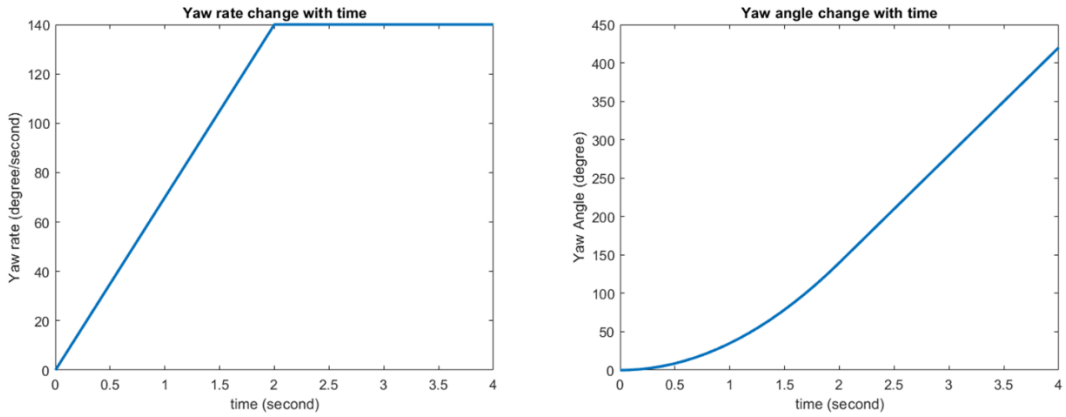

Figure 10: Yaw Outputs of Unsuccessful Manual Control

Finally, the change of the vehicle's direction and position with respect to the Inertial Frame is as in Figure 11.

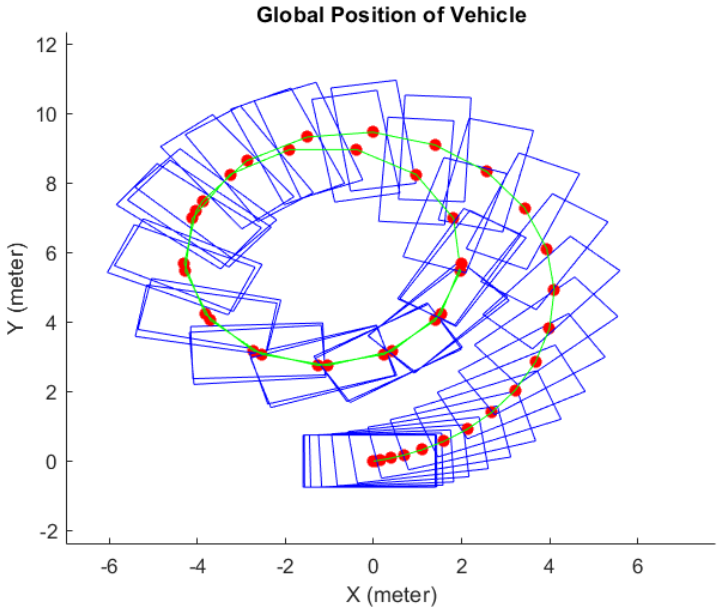

Figure 11: Global Position of Vehicle with Unsuccessful Manual Control

1.2.4 Conclusion

The dynamic model, in which Drag forces, Friction forces and Elastic forces are neglected, provide the desired outputs as open loop manual control with motor torque and steer angle inputs. But the vehicle needs a closed loop controller for autonomous driving. A controller will be designed for the vehicle in the next part.

1.3 Revisions

1.3.1 Dynamic Model Revisions

For a more controllable and realistic vehicle model, the lateral friction applied by the ground to the vehicle during the turn and the longitudinal component of this friction are included in the dynamic equations. Since it is assumed that all of the friction force generated during linear motion provides the thrust power with the torque of the motor, it is not included in the equation as friction force.

Effect of lateral friction during rotation on lateral and longitudinal accelerations, modified version of equation 1.6;

$$\begin{aligned} \frac{d\dot{\psi}}{dt} &= \frac{l_f \tau \delta}{I_{zz} R_f} \\ \frac{dV_y}{dt} &= \frac{\tau \delta}{m R_f} + V_x \dot{\psi} - \mu g \\ \frac{dV_x}{dt} &= \frac{\tau}{m R_f} - V_y \dot{\psi} - \mu g \delta \\ \frac{d\psi}{dt} &= \dot{\psi} \end{aligned} \tag{1.9}$$

μ is friction coefficient and g is gravitational acceleration.

1.3.2 Environment and Vehicle Properties Revisions

In the previous report, the motor constant is specified incorrectly due to an unit conversion error. In addition, with the added friction forces, new parameters for environmental conditions should be explained. Therefore Table 1 has been rearranged;

Table 2: Rearranged Vehicle Properties and Environment Conditions

Features	Values
Mass	$2000\ kg$
Inertia about Z-axis	$4000\ kg/m^2$
Front Axle to Center of Gravity	$1.4\ m$
Rear Axle to Center of Gravity	$1.6\ m$
Radius of front wheel	$0.3\ m$
Motor resistance	$0.02\ ohm$
Motor constant	$100\ Nm/A$
Input Voltage Limits	$[-10V, 10V]$
Input Steer Angle Limits	$[-60°, 60°]$
Gravitational Acceleration	$9.81\ m/s^2$
Asphalt Kinetic Friction Coefficient(in Turkey)	0.8
Asphalt Static Friction Coefficient(in Turkey)	1

2. Part II: Designing Controllers

The system is linearized so that the dynamics of the vehicle can be controlled. Then, control was provided by integrating PID controllers into the linear system.

2.1 System Linearization

The system is nonlinear as stated in equation 1.8. While linearizing the system, the equilibrium point mentality is taken as a base [5]. In order to use such a linearization method, the parameters to be controlled are controlled sequentially. First of all, steer angle input is controlled to provide the desired yaw angle. Then, voltage input is controlled to obtain the desired longitudinal velocity by using the values in the resulting equilibrium state.

2.1.1 Linearization of Rotational Motion Dynamics

Nonlinear equations of rotational motion dynamics;

$$\frac{d\dot{\psi}}{dt} = \frac{l_f k \mathbf{V} \delta}{I_{zz} R_f \Omega}$$
$$\frac{d\psi}{dt} = \dot{\psi} \tag{2.1}$$

l_f, k, I_{zz}, R_f, and Ω values are constant. But voltage and steer angle are variable since they are inputs of the system. For this reason, since no longitudinal control is made during rotation, rotations are made with a fixed voltage value. Considering the characteristics of the vehicle and in order to make the turns more controllable, the voltage value that allows a smooth turn was chosen as 0.05 Volts. Thus, a slow and easy controllable system has been obtained.

Coefficient of rotational motion with constant voltage;

$$C_{Rotational} = \frac{l_f k \mathbf{V}}{I_{zz} R_f \Omega} \tag{2.2}$$

Statement of rotational dynamic system as linear state-space model;

$$\dot{x} = \begin{bmatrix} \ddot{\psi} \\ \dot{\psi} \end{bmatrix} = \begin{bmatrix} 0 & 0 \\ 1 & 0 \end{bmatrix} \begin{bmatrix} \dot{\psi} \\ \psi \end{bmatrix} + \begin{bmatrix} C_{Rotational} \\ 0 \end{bmatrix} \delta$$
$$y = \begin{bmatrix} 1 & 0 \\ 0 & 1 \end{bmatrix} \begin{bmatrix} \dot{\psi} \\ \psi \end{bmatrix} \quad (2.3)$$

2.1.2 Linearization of Linear Motion Dynamics

Nonlinear equations of linear motion dynamics;

$$\frac{dV_y}{dt} = \frac{\mathbf{V}k\delta}{\Omega m R_f} + V_x\dot{\psi} - \mu g$$
$$\frac{dV_x}{dt} = \frac{\mathbf{V}k}{\Omega m R_f} - V_y\dot{\psi} - \mu g\delta \quad (2.4)$$

Since the control is provided in order, while the longitudinal control is done, rotational control has already been made. Therefore, steer angle and yaw rate are zero during longitudinal control. When the equations are rearranged in 2.4 with this information;

$$\frac{dV_y}{dt} = -\mu g$$
$$\frac{dV_x}{dt} = \frac{\mathbf{V}k}{\Omega m R_f} \quad (2.5)$$

Coefficient of linear motion with zero yaw rate and steer angle;

$$C_{Linear} = \frac{k}{\Omega m R_f} \quad (2.6)$$

Statement of rotational dynamic system as linear state-space model;

$$\dot{x} = \begin{bmatrix} \dot{V}_y \\ \dot{V}_x \end{bmatrix} = \begin{bmatrix} 0 & 0 \\ 0 & 0 \end{bmatrix} \begin{bmatrix} V_y \\ V_x \end{bmatrix} + \begin{bmatrix} 0 \\ C_{Linear} \end{bmatrix} \mathbf{V} + \begin{bmatrix} -\mu g \\ 0 \end{bmatrix}$$
$$y = \begin{bmatrix} 1 & 0 \\ 0 & 1 \end{bmatrix} \begin{bmatrix} V_y \\ V_x \end{bmatrix} \quad (2.7)$$

2.2 Design of Controllers

After the system is linearized, it is easier to control. PID is used to control the system. In MATLAB Simulink where the system is modeled, there is a PID tuner application to tune the PID (Proportional, Integral and Differential) gains.

For this reason, PID, which is a traditional and functional control method, has been preferred in order to easily regulate the system response characteristics.

2.2.1 Lateral Controller

Lateral control works to obtain the desired yaw angle.

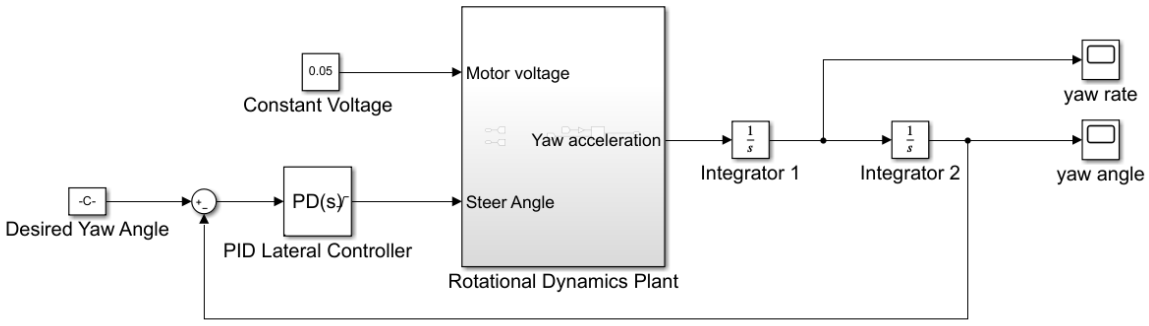

Figure 12: Basic Block Model of Lateral Control

As in the block model in System Figure 12, the PID controller produces steer angle input value by using the amount of error between the yaw angle, which is the response of the dynamic system and the desired yaw angle.

The dynamic model of the model in Figure 12 is given in Figure 13.

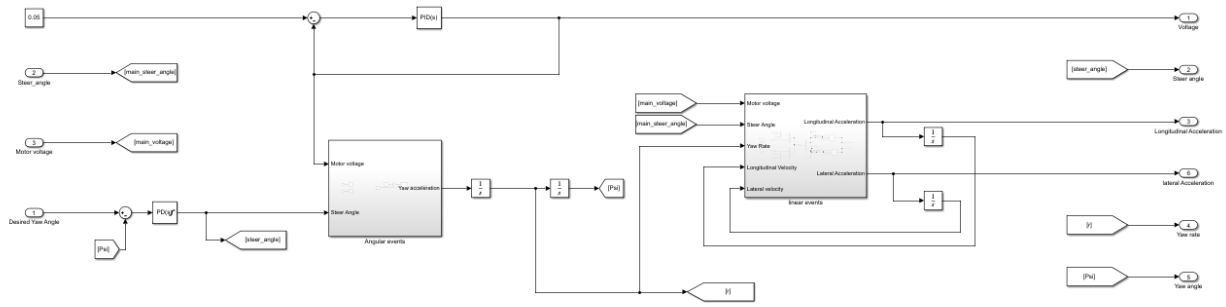

Figure 13: Yaw Angle Control Subsystem (attached in simulation files)

Manual optimization of the gain value obtained using the PID Tuner has been decided to be zero as the integral gain extends the system response time and causes overshoot. Thus, only PD (Proportional and Differential) gains are used in the system. Also, considering the steer angle limits given in Table 2, the PID controller was defined saturation as -60 to 60 degree. The determined gain values are given in Table 3.

Table 3: Lateral Controller Values of PID Gains

Gains	Values
Proportional	1.8429
Integral	0
Differential	3.6241

2.2.2 Longitudinal Controller

Longitudinal control works to obtain the desired longitudinal velocity.

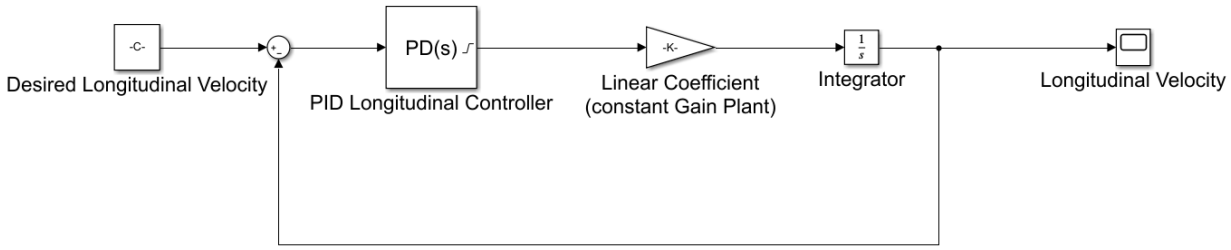

Figure 14: Basic Block Model of Longitudinal Control

As in the block model in System Figure 14, the PID controller produces voltage input value by using the amount of error between the longitudinal velocity, which is the response of the dynamic system and the desired longitudinal velocity.

Similarly, PD controller is used here and considering the voltage limits given in Table 2, the PID controller was defined saturation as -10 to 10 voltages. The determined gain values are given in Table 4.

Table 4: Longitudinal Controller Values of PID Gains

Gains	Values
Proportional	1.2332
Integral	0
Differential	0.0859

2.3 Results

This section will examine how the vehicle's controllers work individually and as a hybrid.

2.3.1 Case I: Lateral Controller Results

Firstly, the desired yaw angle of 50 degrees was defined in the system as step input. A response was obtained from the system with approximately 2% overshoot and 10 seconds settling time. This response and the steer angle input signal generated by the Controller are shown in Figure 15.

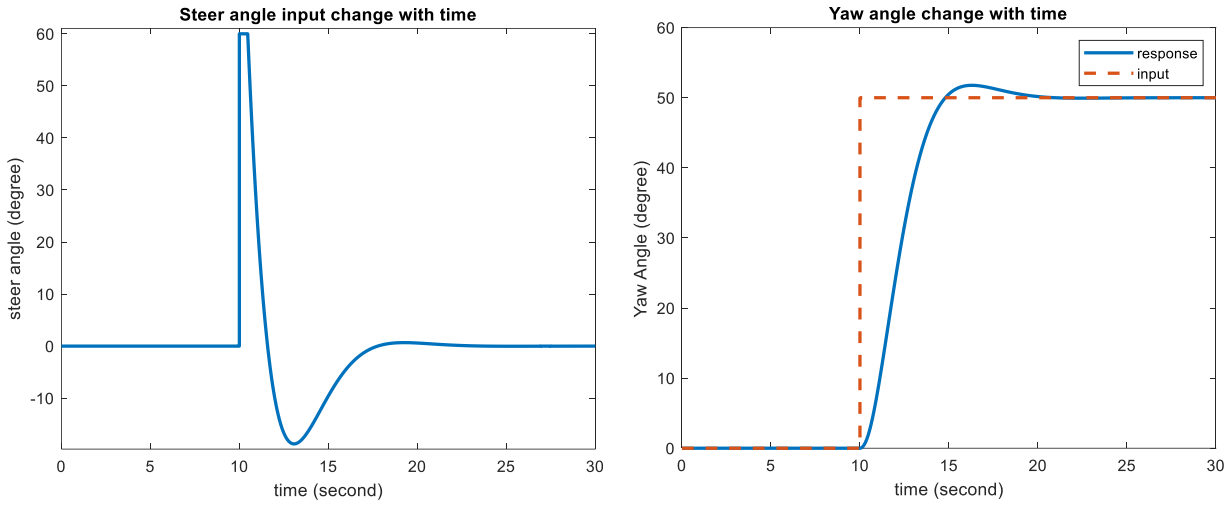

Figure 15: System step response and generated steer angle signal lateral controller

Then, in Figure 16, the response of the system against multistep input was examined. The desired yaw angle values, respectively; it changed to 0, 80, -120 and -50 degrees.

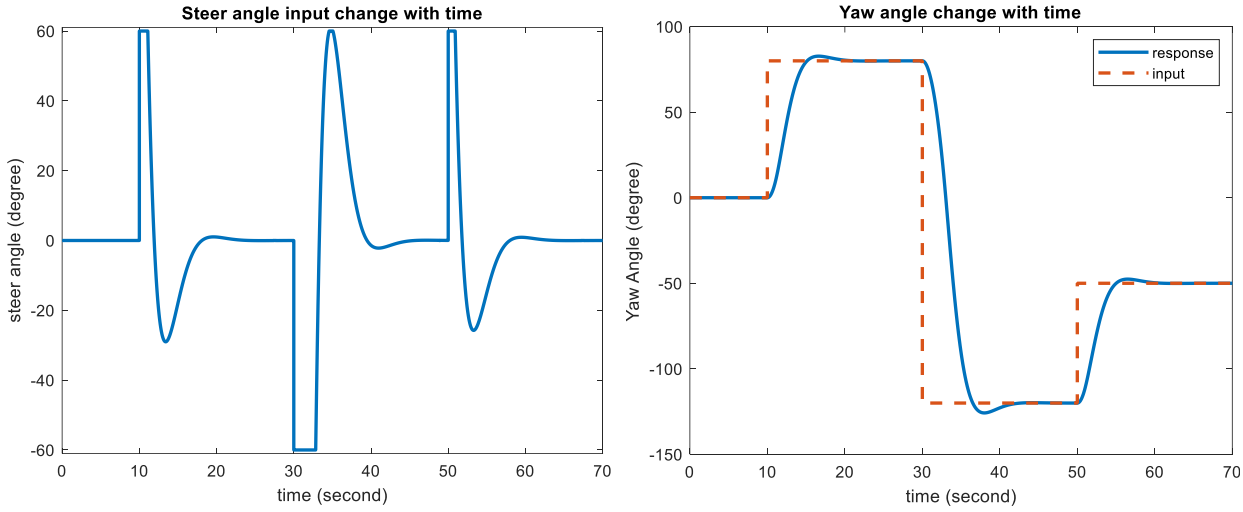

Figure 16: System multistep response and generated steer angle signal lateral controller

In Figure 17, the desired yaw angle is defined as ramp input from 0 to 80.

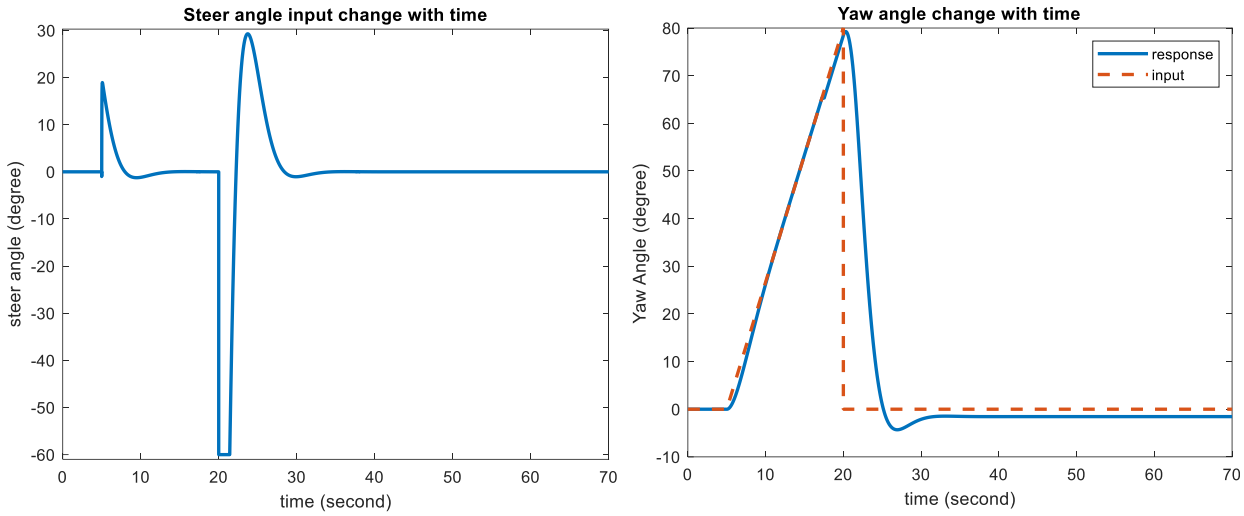

Figure 17: System ramp response and generated steer angle signal by lateral controller

The vehicle's responses are not as abrupt as expected, so the vehicle will not lose control during path tracking (Chapter 3). Thanks to the linearization of the system, it is easily controlled as a constant voltage value is applied during the control (Linearization: Chapter 2.1).

2.3.2 Case II: Lateral Controller results

After linearization, longitudinal control is much easier than lateral control. Because the control process takes place sequentially. After the rotation is completed, the steer angle and yaw rate that affect the longitudinal velocity become zero and can be easily controlled by only voltage input. For this reason, a fast response system has been designed.

Firstly, the desired longitudinal velocity of 100 km/h was defined in the system as step input. A response was obtained from the system with zero overshoot and 2 seconds settling time. This response and the voltage input signal generated by the controller are shown in Figure 18.

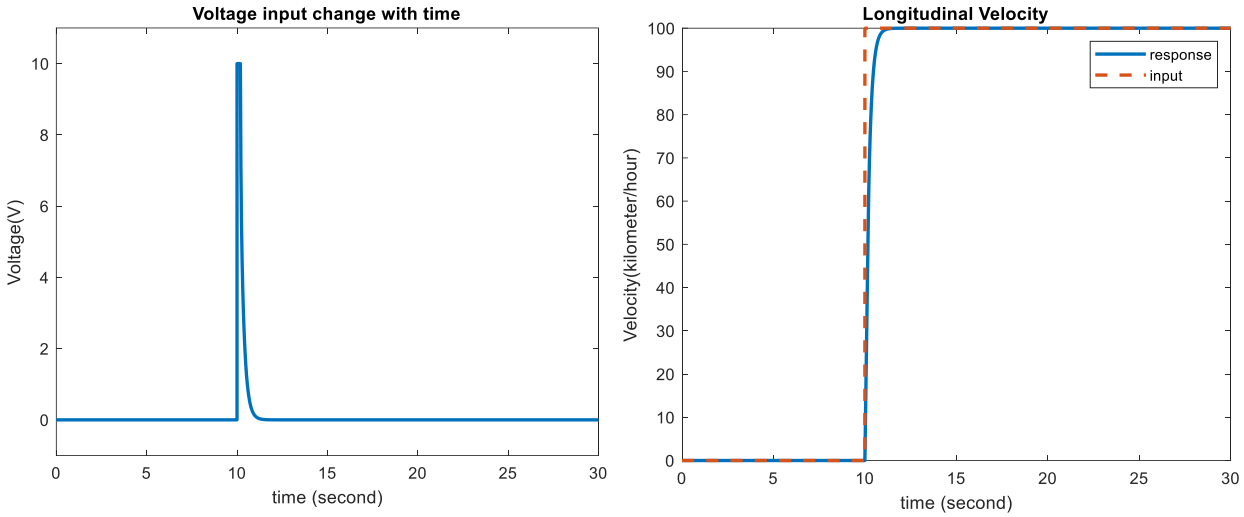

Figure 18: System step response and generated voltage signal by longitudinal controller

Then, in Figure 19, the response of the system against multistep input was examined. The desired longitudinal velocity values, respectively; it changed to 0, 100, 50 and 60 kilometers per hour.

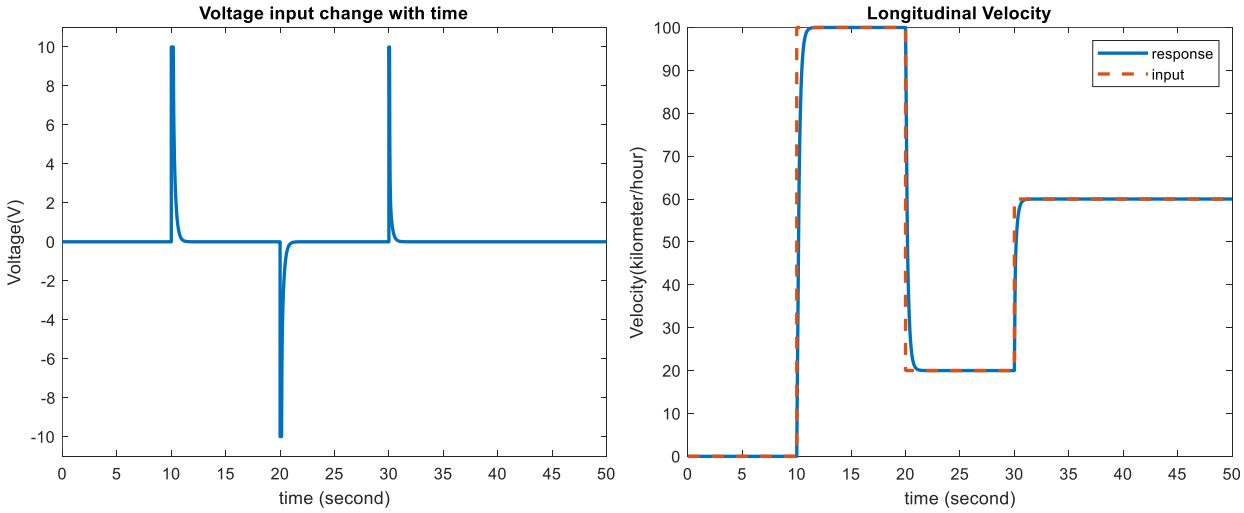

Figure 19: System multistep response and generated voltage signal by longitudinal controller

In Figure 20, the desired longitudinal velocity is defined as ramp input from 0 to 100 km/h.

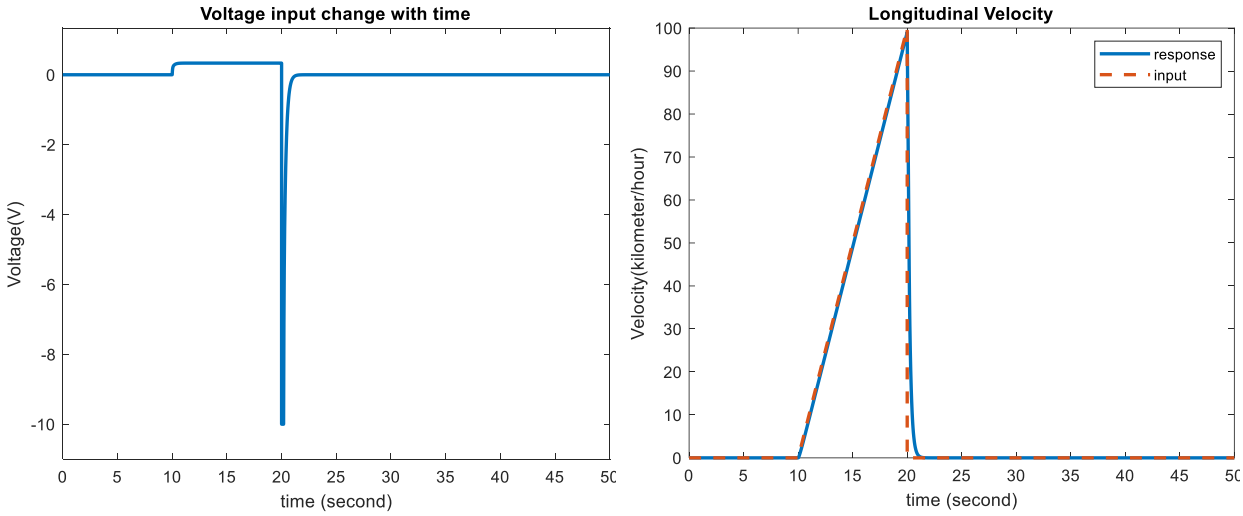

Figure 20: System ramp response and generated voltage signal by longitudinal controller

As mentioned at the beginning of the section, control of longitudinal velocity became very easy after linearization. The results also support this situation.

2.3.3 Case III: Hybrid Control Results

In this section, the results are examined by running two controllers together. Since the system will be controlled sequentially, the longitudinal velocity response is expected to occur after the yaw angle response is completed.

When 100 km / h longitudinal velocity and 50 degrees yaw angle are inputted into the system, the response of the system is given in figure 21 and the steer angle and voltage input signal produced by the controller is included in the figure 21.

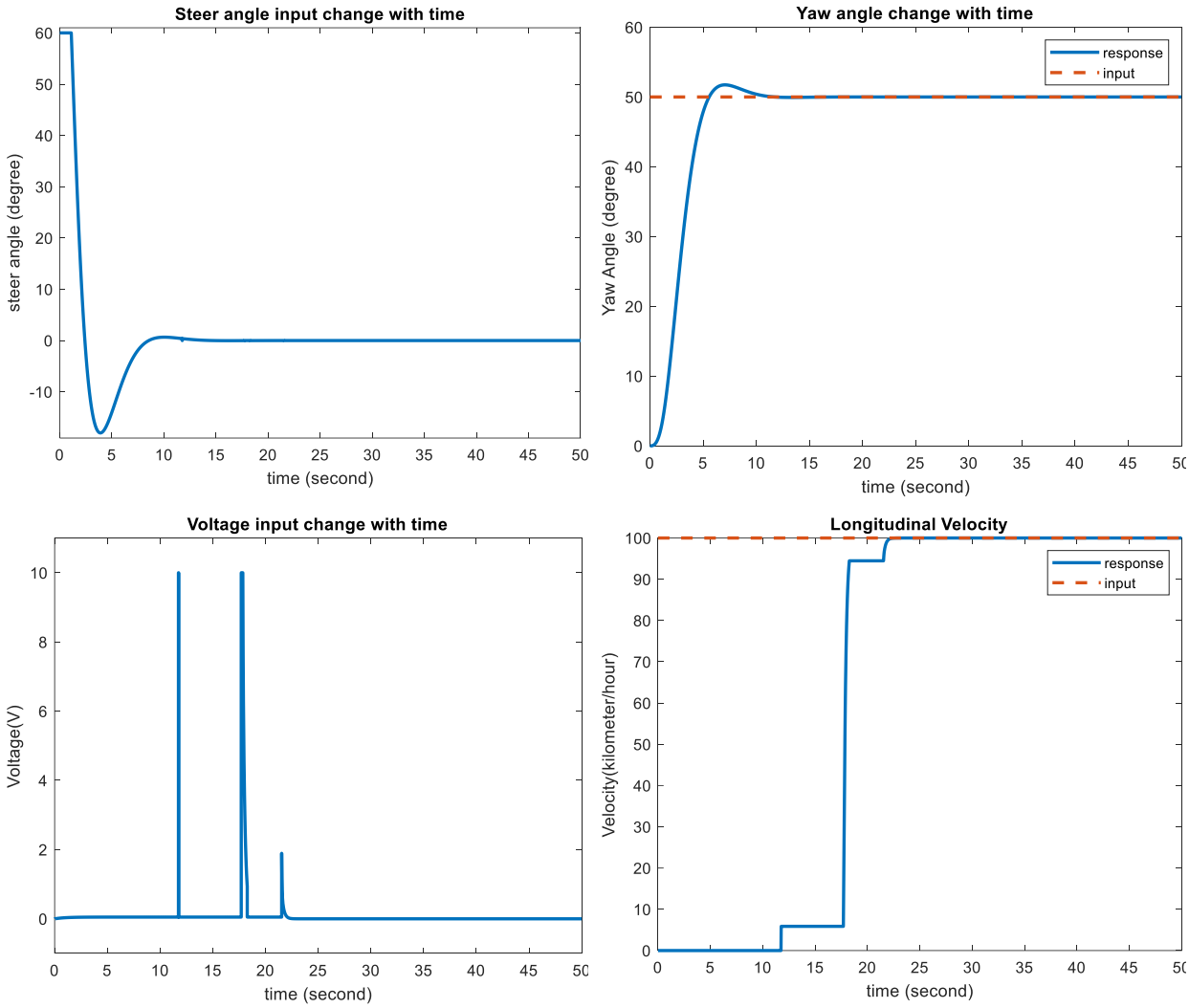

Figure 21: Hybrid control results and inputs

As shown in the figure, longitudinal velocity is not controlled until yaw angle is controlled. After controlling the yaw angle, the longitudinal velocity was controlled to increase to the desired value.

3. Part III: Path Planning, Path Managing and Executing Pre-Determined Scenarios

In this section, as can be understood from the title, calculations and scenarios related to the path will be explained.

3.1 Path Planning

In the path planning algorithm written for this study, the user manually enters the waypoints to be visited. Waypoint matrices are 1x5 in size.

$$Waypoint\ Matrix = [X_{target}, Y_{target}, V_{desired}, \Delta t_{waiting}, Diameter_{desired}] \quad (3.1)$$

The first element of the matrix is the X axis of the target point.

The second element of the matrix is the Y axis of the target point.

The third element of the matrix is the desired longitudinal velocity.

The fourth element of the matrix is the amount of time to wait on the target.

The fifth element of the matrix is the diameter of the circle for turning around the target.

They are determined by the user.

If the waiting time is greater than zero, the path planning algorithm defines an extra point. This point is a point slightly behind the target point and the vehicle slows down when it gets here. Thus, it minimizes its distance from the point where it will stop. This situation is shown in figure 22.

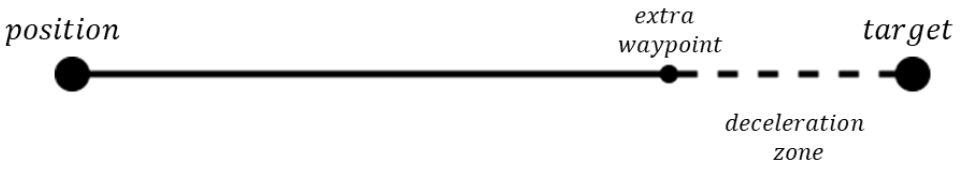

Figure 22: Extra point determined by Path Planning Algorithm for Deceleration

If the vehicle is required to rotate around a waypoint, that is, if the turn diameter input is greater than zero, the Path Planning algorithm defines a total of 24 extra waypoints at 15 degrees intervals at a radius distance to the target point. Thus, the vehicle follows the waypoints and draws a circle. In addition, when it will turn, it slows down its speed and thus a successful turn is made without being thrown.

3.2 Path Managing

The vehicle uses the Atan2 function to compensate for the yaw angle difference between the target to head towards and its own position when heading towards the target. This function calculates the angle between the target point and the instantaneous position using an arctangent by controlling its sine and cosine. The function is the statement to obtain the required yaw angle as follows [6];

$$\Delta\psi_{required} = atan2(Y_{target} - Y, X_{target} - X) \qquad (4.2)$$

In the path manager system, each waypoint has a number in order. If the distance with the desired waypoint falls below one meter, the waypoint counter in the Path manager system increases by one. Thus, the tool uses equation 3.2 again to head to the next waypoint.

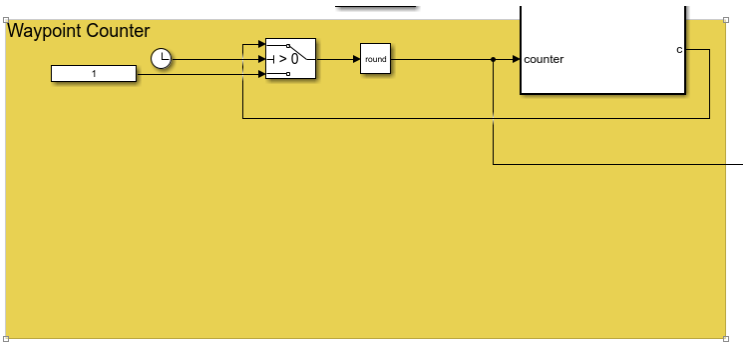

Figure 23: Waypoint Counter Simulink Block Diagram

If the desired waiting time for the Waypoint is greater than zero, the time counter resets and starts counting time again, and it gives the longitudinal controller the desired velocity information 'zero' until the desired waiting time is reached. Time counter input and outputs shown in Figure 24.

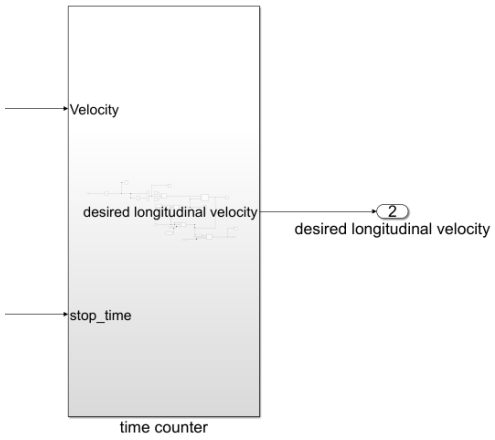

Figure 24: Time Counter Subsystem with Inputs and Output

When the final waypoint is reached, the Path manager system finishes the simulation.

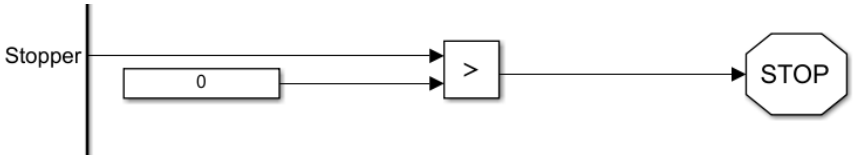

Figure 25: Simulation Stopper System

If the waypoint counter is greater than the number of waypoints, it means that the last waypoint has been reached. Thus, the logical input stopper becomes equal to one and stops the simulation.

3.3 Executing Pre-determined Scenarios

In this section, the desired tasks were made by vehicle by using Path Planning and Path Managing methods, which have been explained so far.

3.3.1 Case I: Going from A to B

The starting point of the vehicle in this and other missions is A = (0, 0). In this task, the vehicle was requested to go to point B = (200, 400).

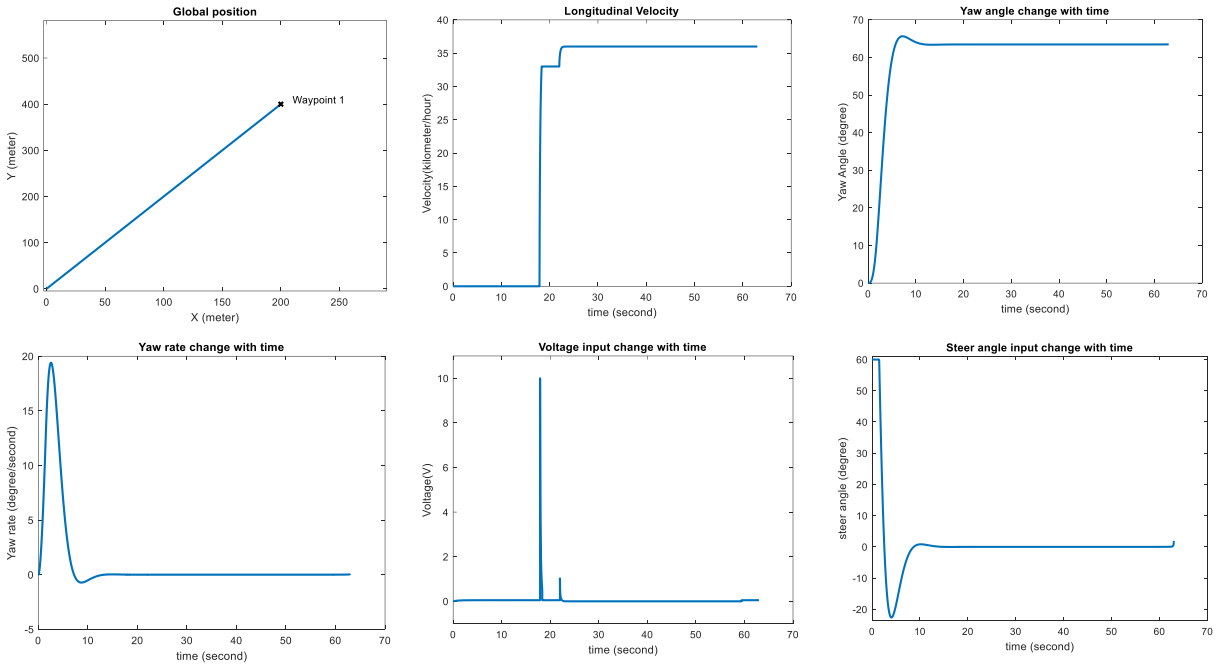

Figure 26: Task I Simulation Graphs

The results of this basic task in Figure 26 show the vehicle's success in steering and moving forward. 36 km / h was input to the vehicle as the desired velocity. Since the vehicle did not make sudden movements, the lateral acceleration remained zero throughout the movement as it could not overcome the static friction.

3.3.2 Case II: Waiting at the Waypoints

Mission requirements;

- Go A=(0, 0) to B=(200, 400) and Stay at point B for 60 seconds
- Go B=(200,400) to C=(1000, 1100) and Stay at point C for 30 seconds
- Go C=(1000, 1100) to D=(2000, 300) and do not Stay at point D
- Go D=(2000, 300) to E=(1000, 0) and stop simulation

Task waypoints have been entered into the system together with the desired waiting time values.

The change in position is given in Figure 27. At the points where the vehicle stopped and moved again, it was able to make a sharper turn because its speed was slow. The vehicle's stop points attached in Figure 27. It was able to stand at points B and C (Waypoint 1 and 2) about 15 meters away. The reason for this is that the speed of the vehicle cannot suddenly be zero during deceleration.

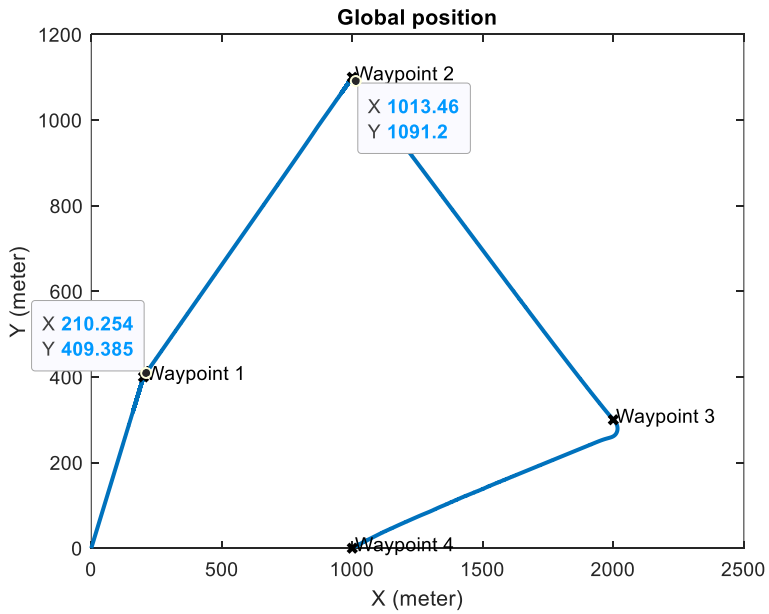

Figure 27: Task II global position Graph

When the system gives the stop command to the vehicle, the speed becomes zero. The areas where the speed is zero, that is, the vehicle is waiting for, are shown in red in the Velocity graph, in Figure 28. It is also clearly seen that the vehicle slows down as it approaches the point of stopping.

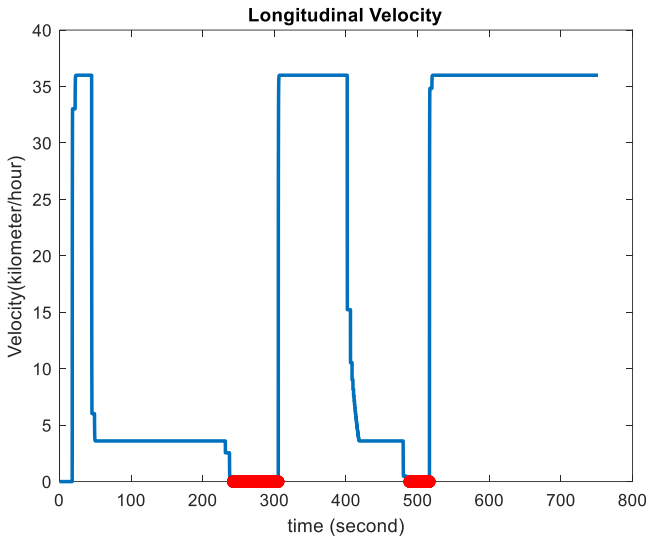

Figure 28: Task II Longitudinal Velocity Graph (waiting times are red)

As in the previous task, the lateral velocity remained zero in this mission as it could not overcome friction. Also, yaw angle change is given in figure 29.

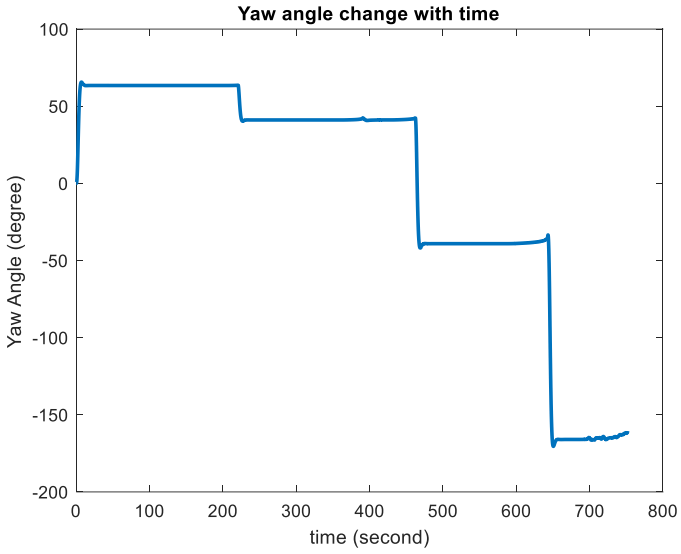

Figure 29: Task II Yaw Angle Graph

3.3.3 Case III: Obeying Speed Limit Rules

Mission requirements;

- Go A= (0, 0) to B= (200, 400) with max. 90 km/h velocity.
- Go B= (200,400) to C= (1000, 1100) with max. 30 km/h velocity
- Go C= (1000, 1100) to D= (2000, 300) with max. 110 km/h velocity
- Go D= (2000, 300) to E= (3000, 500) with max. 120 km/h velocity

Task waypoints have been entered into the system together with the desired velocity values.

The autopilot system of the vehicle works by obtaining the desired speed value instead of limiting the speed. In addition, since the longitudinal controller does not cause any overshoot, maximum limits are inputted in the system as desired velocities. Velocity graph attached in Figure 30.

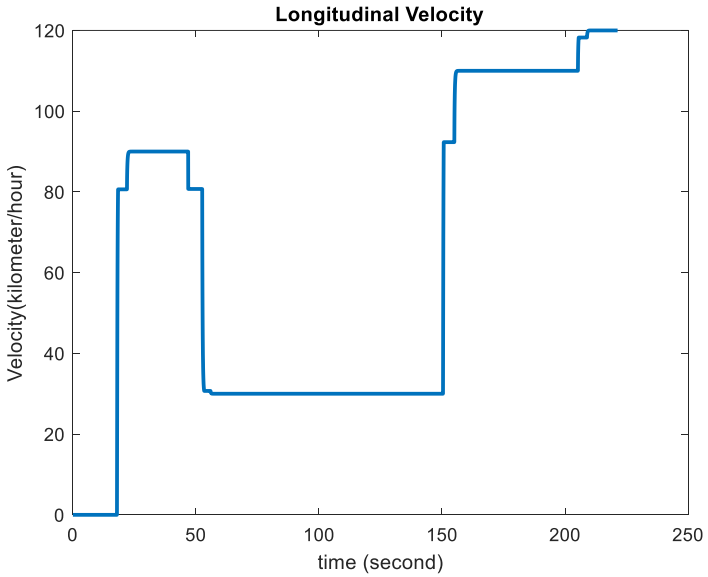

Figure 30: Task III Velocity Graph

As mentioned, the system can move at the desired speed by complying with the speed limits. Other results of the task are included in Figure 31.

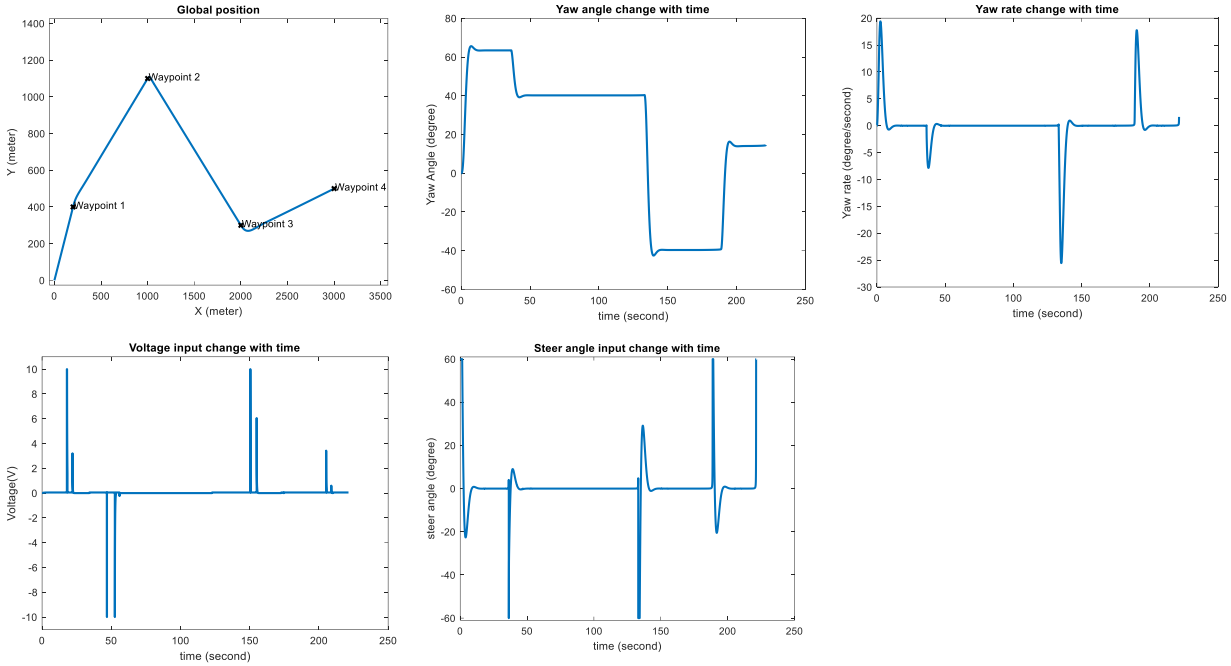

Figure 31: Task III Simulation Graphs

As can be seen from the other results, the vehicle does not have any problems in changing its speed.

3.3.4 Case IV: Circular Rotation Motion

In this task, it is requested to make a circular motion with a diameter of 30 meters around B = (200,400). While performing the task, the Path planning algorithm creates an extra set of points to provide circular motion, as mentioned in section 3.2. The position graph obtained after the simulation and the zoomed version is shown in figure 32.

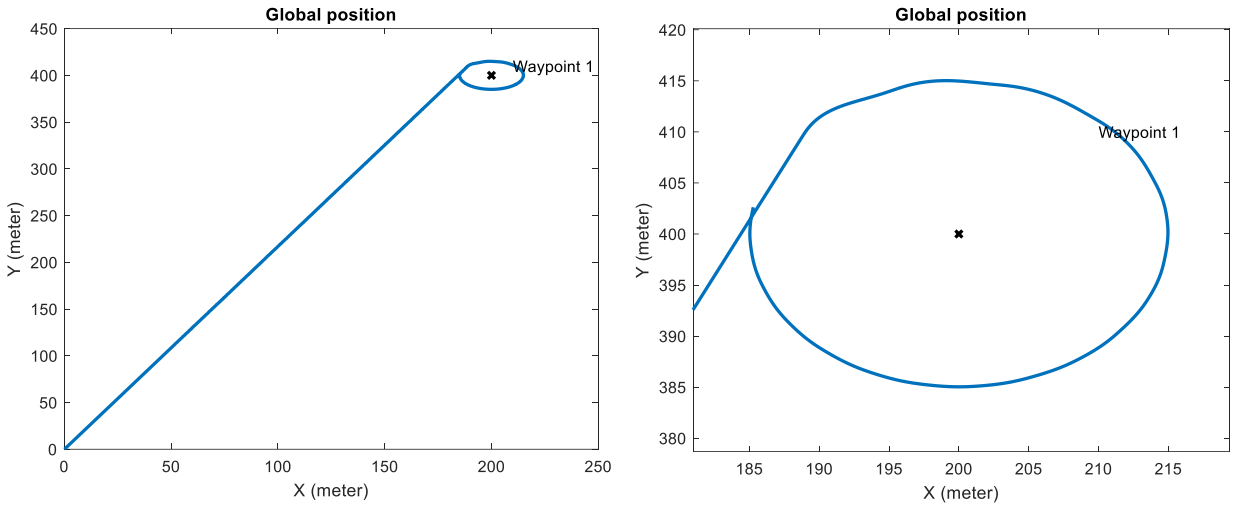

Figure 32: Task III Global Position Graphs

Although the vehicle swayed a little when it first started to turn, its movement improved afterwards. During the rotation, the yaw angle changes linearly as expected. It is given in Figure 33 with the steer angle and Yaw rate changes.

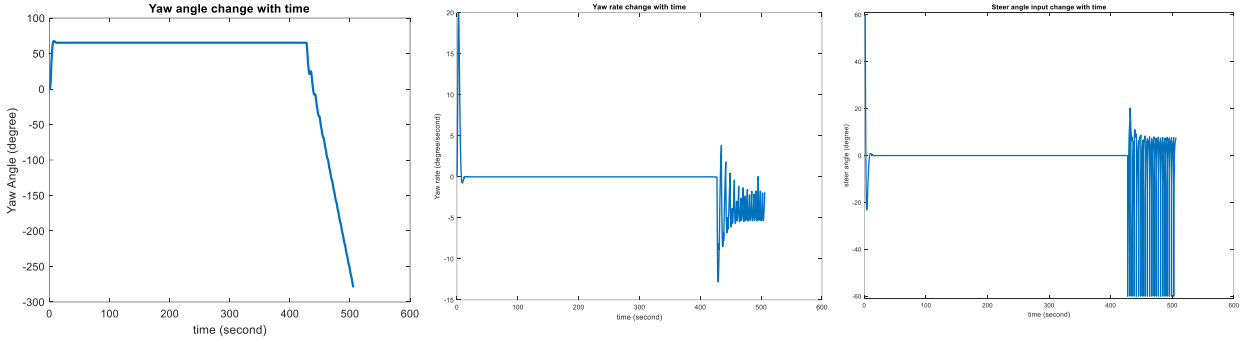

Figure 33: Task IV Angular results

Steer angle inputs of the vehicle change very suddenly while the vehicle is turning. In fact, since such a situation is likely to damage the vehicle, various corrections can be made to the rotation control of the system.

4. Conclusion

In this study, the dynamics of an autonomous land vehicle are modeled, its longitudinal and lateral controllers have been designed and a path planing process has been applied. The results were given graphically and necessary explanations were made. The vehicle has successfully completed its missions.

Path planning algorithm in the study was written in MATLAB. Dynamics are modeled with MATLAB Simulink. The simulation files are attached. General view of the model is given in Figure 34.

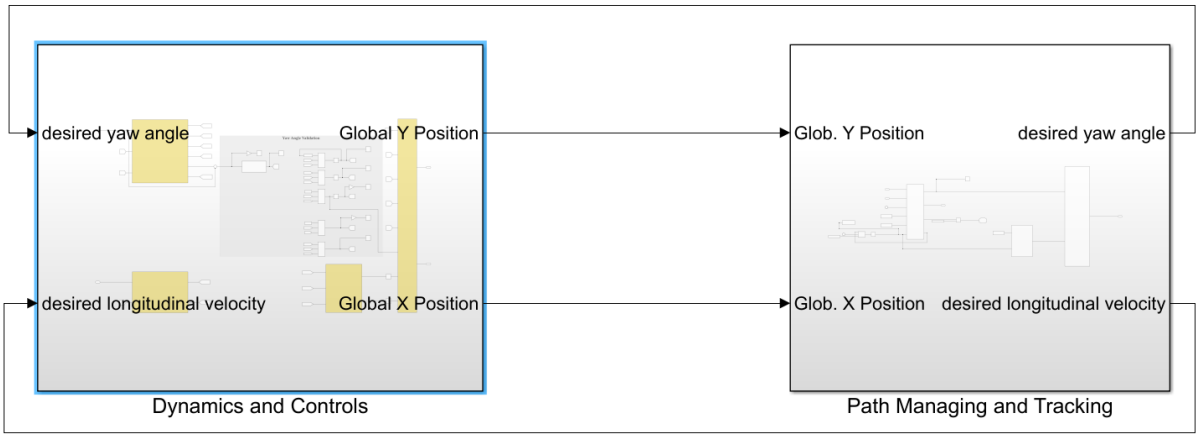

Figure 34: General View of Vehicle Model

References

[1]Popp, K., Schiehlen, W., Kröger, M., & Panning, L. (2010). "*Ground vehicle dynamics" (p. 165)*. Berlin: Springer. doi:10.1007/978-3-540-68553-1.

[2] Radionova L.V., Chernyshev A.D., (2015). "*Mathematical model of the vehicle in MATLAB Simulink".* South Ural State University, 76, Lenin Avenue, Chelyabinsk, 454080, Russian Federation. doi: 10.1016/j.proeng.2015.12.114

[3]PP. Ramata, (2010). "*Vehicle Dynamic Modeling " (Chapter 2, p.17,25)*. Virginia Tech University. Retrieved from https://vtechworks.lib.vt.edu/bitstream/handle/10919/36615/Chapter2a.pdf?sequence=4

[4]D. Collins, (2017). "*The Torque Equation and the Relationship with DC Motors"*.Motion Control Tips (e-Article). Retrieved from https://www.motioncontroltips.com/torque-equation/

[5]R. Murray, J. Hauser (1991). "*A Case Study in Approximate Linearization: The Acrobot Example "(p. 8, Chapter 3)*. Electronics Research Laboratory, University of California, Berkeley, CA 94720.

[6]R. Beard, T. McLain (2012). "*Small Unmanned Aircraft"(p. 180)*. Princeton University Press, 41 William Street, Princeton, New Jersey 08540